

Electronic supplementary information (ESI)

Application of the Ni and Cu-MOFs as highly efficient catalyst for visible light-driven tetracycline degradation and hydrogen production

Qigao Shang^{a,b}, Nannan Liu^a, Dan You^b, Qingrong Cheng^{a,*}, Guiying

Liao^b, Zhiquan Pan^a

^a Key Laboratory for Green Chemical Process of Ministry of Education, Wuhan Institute of Technology, Wuhan 430073, P. R. China

^b Engineering Research Center of Nano-Geo Materials of Ministry of Education, China University of Geosciences, Wuhan 430074, P. R. China.

Corresponding authors:

*(Q.C.) E-mail: chengqr383121@sina.com

Total number of pages: 7

Total number of Tables: 4

Total number of Figures: 5

Physical Measurements.

The crystal data were collected on a Bruker SMART APEX CCD diffractometer with graphite-monochromated Mo K α radiation ($\lambda = 0.71073 \text{ \AA}$) using the SMART and SAINT programs. The structure was processed by direct methods and refined on F² by full-matrix least-squares methods with SHELXTL version 5.1. Nonhydrogen atoms of the ligand backbones were refined anisotropically. All the hydrogen atoms of the TIB backbones were fixed geometrically at calculated positions and allowed to ride on the parent non-hydrogen atoms. Details of the crystallographic data of 1 and 2 are summarized in Table S1. FT-IR spectra (KBr pellets) were recorded on a Perkin-Elmer GX FTIR spectrometer in the region 4000–450 cm⁻¹. CHN analyses were done using elemental vario MICRO CUBE analyzer. UV-vis diffuse reflectance spectra (DRS) were tested on a PerkinElmer Lambda2S spectrophotometer, in the range of 200–800 nm in the solid state. The UV-vis spectra for MB solution were measured on a Shimadzu UV 2450 spectrometer (UV-3600, Shimadzu, Japan). Powder X-ray diffraction (PXRD) patterns were collected using a PANalytical Empyrean (PIXcel 3D detector) system with CuK α radiation ($\lambda = 0.15418 \text{ nm}$), and the 2θ range of 5–80°. The X-ray photoelectron spectra (XPS) were recorded on an ESCALAB250 spectrometer (Thermo-VG Scientific) using MgK α radiation (1253.6 eV) and the binding energy values were calibrated with respect to the C (1s) peak (284.6 eV). Thermogravimetric analysis (TGA) test were recorded on TG-DTA 2010S MAC apparatus under N₂ atmosphere in the temperature range 40–900 °C with a heating rate of 10°C min⁻¹. Photocatalytic experiments: 300 W ceramic metal halide lamp (PerkinElmer) with 420 nm optical filter. The electron spin resonance (ESR) spectra were detected using a Bruker EPR A 300-10/12 spectrometer to measure the activated species. The mineralization of TC was explored with three-dimensional excitation-emission matrix fluorescence spectroscopy (TOC-L, Shimadzu, Japan). ICP-OES results were obtained on Optima 5300DV from Perkin Elmer.

Table S1. Crystallographic data for complexes **1** and **2**.

Complex	1	2
formula	C ₇₂ H _{81.94} Cu ₃ N ₃₀ O _{22.97}	C ₃₆ H ₃₆ N ₁₄ NiO ₆
CCDC deposit no	1882306	1882332
Formula weight	1925.75	819.50
Crystal system	triclinic	triclinic
Space group	P -1	P -1
a (Å)	9.0707(5)	9.3301(11)
b (Å)	12.9246(6)	9.7106(10)
c (Å)	18.4560(9)	12.7384(12)
α (deg)	82.010(2)	68.712(3)
β (deg)	84.977(2)	69.729(3)
γ (deg)	72.605(2)	64.134(4)
V(Å³)	2042.27(18)	942.97(18)
Z	1	1
D_{calcd}(g cm⁻³)	1.566	1.443
F(000)	995.0	426.0
H,k,l max	10,15,22	11,11,15
Mu(Mo-Kα)[mm⁻¹]	0.869	0.581
Temp , k	173	173
Nref,Npar	7403, 665	3416, 334
R₁ ,wR₁	0.0503, 0.1131	0.0707, 0.1184
S	1.045	1.059

Table S2. Selected bond distances (Å) and angles (°) for complexes **1** and **2**.

Complex1					
bond lengths (Å)		bond angles (°)		bond angles (°)	
Cu1-N4	1.995(3)	N4-Cu1-N10	90.68(12)	N8-Cu2-N8	180.0(3)
Cu1-N10	2.009(3)	N4-Cu1-N14	173.71(13)	N4-Cu1-O10	91.40(12)
Cu1-N14	2.012(3)	N10-Cu1-N14	90.69(12)	N10-Cu1-O10	89.79(12)
Cu1-N12	2.025(3)	N4-Cu1-N12	90.72(12)	N14-Cu1-O10	94.75(12)
Cu1-O10	2.329(3)	N10-Cu1-N12	177.36(12)	N12-Cu1-O10	92.41(12)
Cu2-N6	1.979(3)	N14-Cu1-N12	87.68(12)	N6-Cu2-N6	180.0(2)
Cu1-O4	2.732	Cu2-O1	2.639	N6-Cu2-N8	89.198(111)
N8-Cu2	1.996(3)				

Complex2					
bond lengths (Å)		bond angles (°)		bond angles (°)	
N2-Ni1	2.131(3)	N6-Ni1-N6	180.00	N6-Ni1-N4	86.44(14)
N4-Ni1	2.127(4)	N2-Ni1-N2	180.00	N4-Ni1-N4	180.00
N6-Ni1	2.120(4)	N6-Ni1-N2	92.87(13)	N4-Ni1-N2	87.36(13)

Figure S1. FTIR spectra of complex 1.

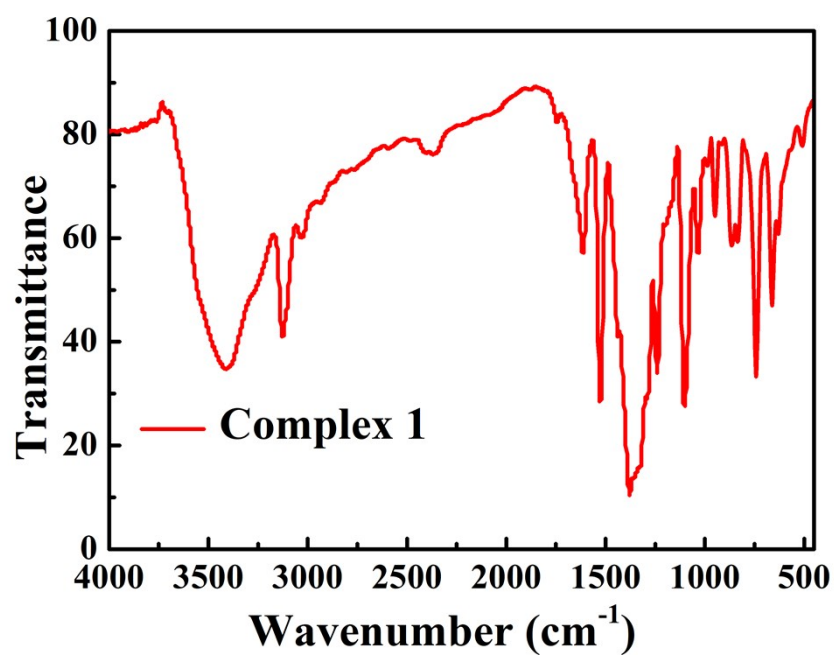


Figure S2. FTIR spectra of complex 2.

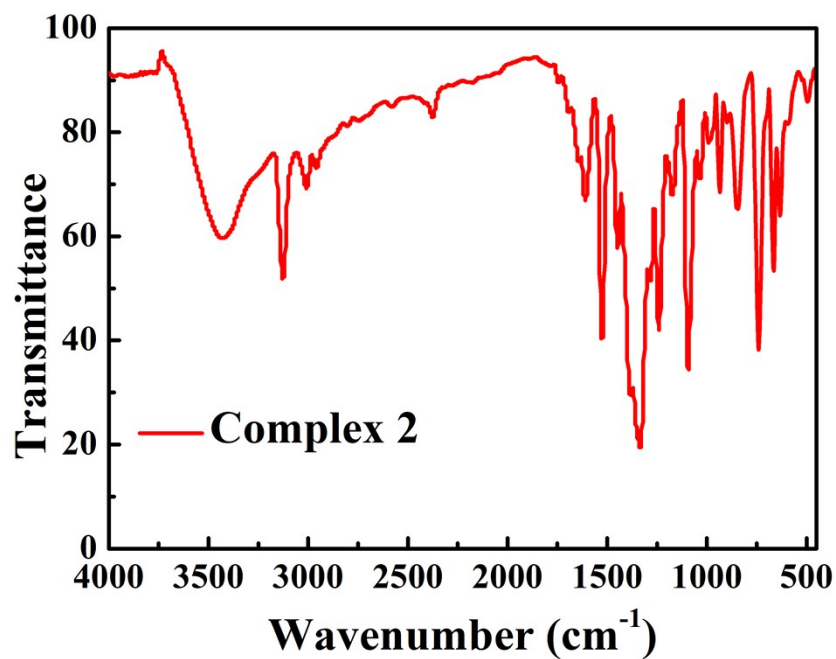


Figure S3. TGA, DSC and DTG curves of complex 1.

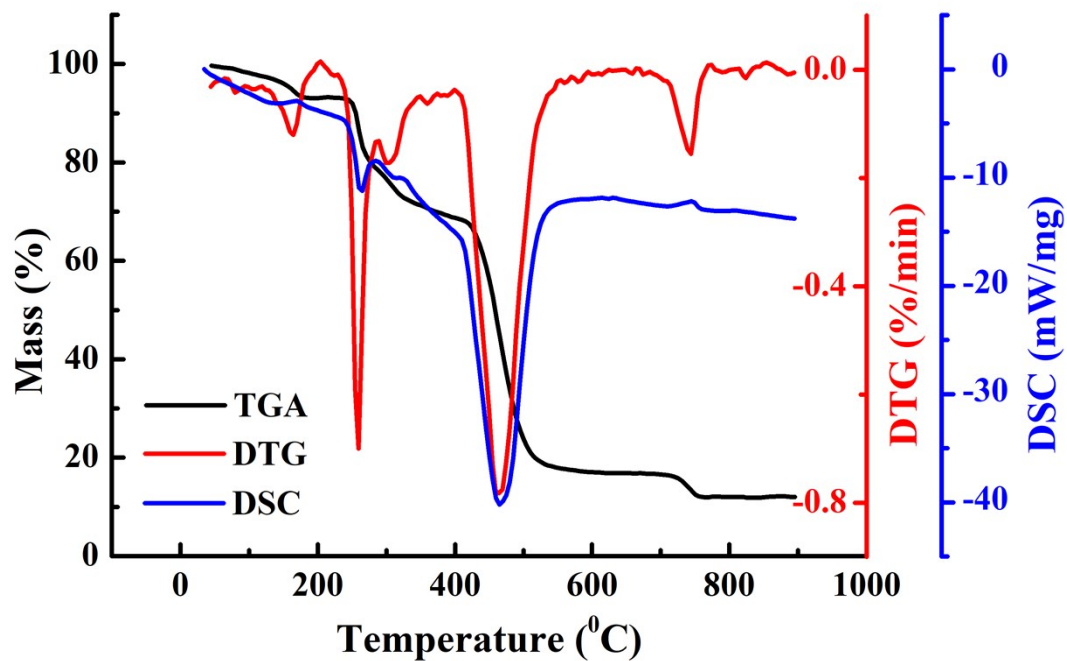
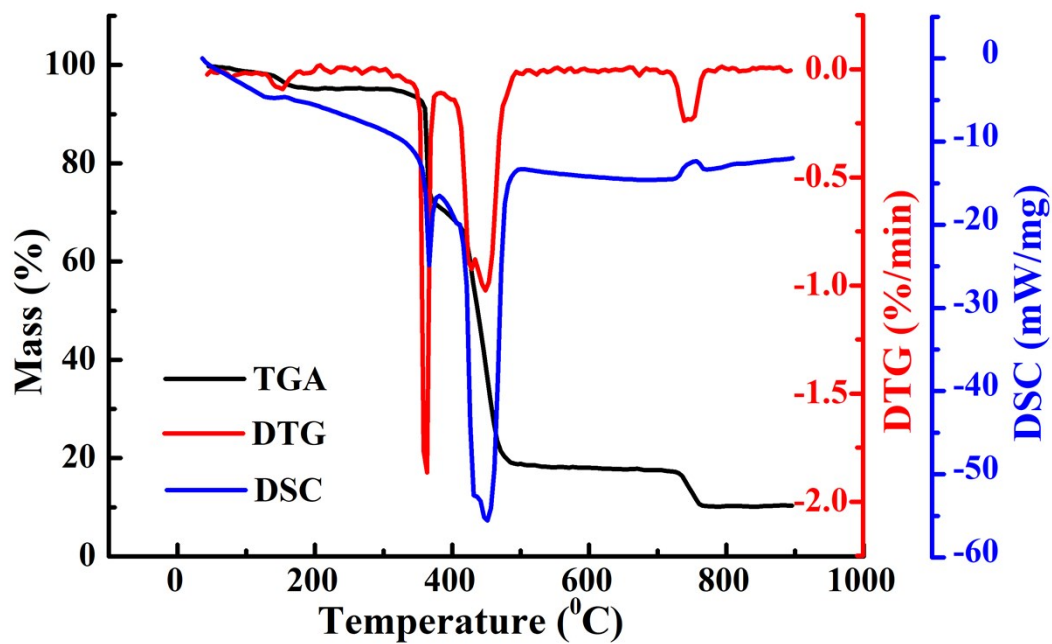


Figure S4. TGA, DSC and DTG curves of complex 2.



Scheme S1. A schematic illustration of photodegradation of TC and photocatalytic H₂ production over complexes **1** and **2**.

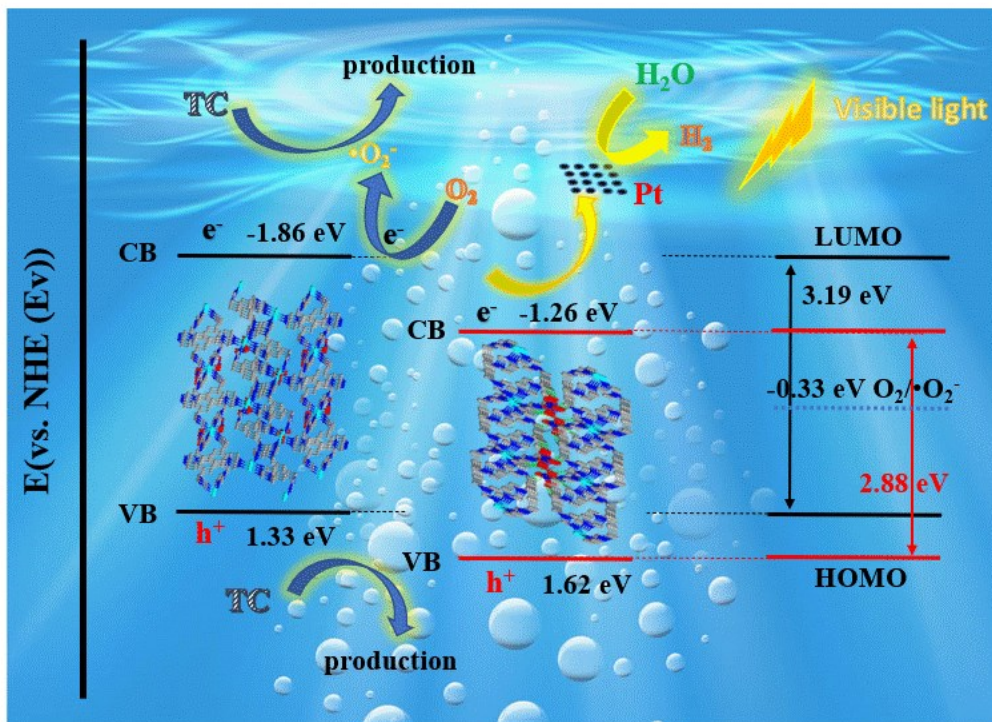


Table S3. Specific surface areas, pore volumes and mean pore diameters for all samples.

<i>Sample</i>	<i>Complex 1</i>	<i>Complex 2</i>
<i>BET surface area</i>	5.49 m ² /g	8.54 m ² /g
<i>Pore size (BJH)</i>	8.49 nm	6.21 nm
<i>Pore size (D-H)</i>	7.75 nm	5.63 nm
<i>Pore volume (cm³ g⁻¹)</i>	0.015 cm ³ /g	0.013cm ³ /g

Table S4. The ICP-OES result of center metal ions concentration in TC aqueous solution after photocatalysis.

<i>System</i>	<i>ICPMS result (mg/L)</i>	<i>Removal rate (%)</i>
<i>Complex 1 (Cu²⁺)</i>	1.94	1.96
<i>Complex 2 (Ni²⁺)</i>	0.02	0.02

Photocatalyst: 50mg: TC:50 mL, 30 ppm.